

Rapid emplacement of massive Duluth Complex intrusions within the Midcontinent Rift

Nicholas L. Swanson-Hysell¹, Steven A. Hoaglund², James L. Crowley³, Mark D. Schmitz³, Yiming Zhang¹, James D. Miller Jr.²

¹ Department of Earth and Planetary Science, University of California, Berkeley, CA, USA

² Department of Earth and Environmental Sciences, University of Minnesota, Duluth, MN, USA

³ Department of Geosciences, Boise State University, Boise, ID, USA

ABSTRACT

The Duluth Complex is one of the largest mafic intrusive complexes on Earth. It was emplaced as the Midcontinent Rift developed in Laurentia's interior during an interval of magmatism and extension from *ca.* 1109 to 1084 Ma. This duration of magmatic activity is more protracted than is typical for large igneous provinces interpreted to have formed from decompression melting of upwelling mantle plumes. While the overall duration was protracted, there were intervals of more voluminous magmatism. New $^{206}\text{Pb}/^{238}\text{U}$ zircon dates for the anorthositic and layered series of the Duluth Complex constrain these units to have been emplaced *ca.* 1096 Ma in less than one million years (duration of $500,000 \pm 260,000$ years). Comparison of paleomagnetic data from these units with Laurentia's apparent polar wander path supports this interpretation. This rapid emplacement bears similarities to the geologically short duration of well-dated large igneous provinces. These data support hypotheses that call upon the co-location of lithospheric extension and anomalously hot upwelling mantle. This rapid magmatic pulse occurred more than 10 million years after initial magmatism following more than 20° of latitudinal plate motion. A likely scenario is one in which upwelling mantle encountered the base of Laurentian lithosphere and flowed via "upside-down drainage" to locally thinned lithosphere of the Midcontinent Rift.

¹⁷ INTRODUCTION

¹⁸ The Midcontinent Rift represents a protracted tectonomagmatic event in the interior of Laurentia
¹⁹ (the North American craton). Voluminous outpouring of lava and emplacement of intrusions
²⁰ accompanied rift development (Fig. 1). Magmatic activity initiated *ca.* 1109 Ma and continued
²¹ until *ca.* 1084 Ma (Swanson-Hysell et al., 2019). Preserved thicknesses of the volcanic successions
²² range from nearly 10 km for partial sections exposed on land, (Green et al., 2011), to ~25 km
²³ under Lake Superior (Cannon, 1992). These volcanics and associated intrusions are much more
²⁴ voluminous than is typical for tectonic rifting. Analysis of seismic data leads to an estimate that
²⁵ total eruptive volume exceeded 2×10^6 km³ with a greater volume added to the lithosphere as
²⁶ intrusions and a magmatic underplate (Cannon, 1992). The ~25 Myr duration of Midcontinent
²⁷ Rift volcanism is much longer than is typical for large igneous province emplacement associated
²⁸ with decompression melting of an upwelling mantle plume. Well-dated large igneous provinces,
²⁹ such as the Central Atlantic Magmatic Province (Blackburn et al., 2013), the Karoo-Ferrar large
³⁰ igneous province(Burgess et al., 2015), and the Deccan Traps (Schoene et al., 2019; Sprain et al.,
³¹ 2019) have durations of <1 Myr for the bulk of their magmatism. An explanation for prolonged
³² volcanism in the Midcontinent Rift could attribute rift initiation and initial volcanism to plume
³³ arrival with continued volcanism resulting from rift-driven asthenospheric upwelling. However,
³⁴ the most voluminous period of magmatism occurred more than 10 million years after initial flood
³⁵ volcanism during an interval known as the “main magmatic stage” (Vervoort et al., 2007). Main
³⁶ stage magmatism has been attributed to an upwelling mantle plume based on the large volume
³⁷ and geochemical signatures (Nicholson and Shirey, 1990; White and McKenzie, 1995).

³⁸ Pioneering Midcontinent Rift geochronology utilized $^{207}\text{Pb}/^{206}\text{Pb}$ dates on zircon from
³⁹ volcanics (Davis and Green, 1997) and intrusions (Paces and Miller, 1993) to illuminate the
⁴⁰ magmatic history. Subsequent advances in U-Pb geochronology enable higher precision
⁴¹ $^{206}\text{Pb}/^{238}\text{U}$ dates to be used when chemical abrasion methods have mitigated Pb loss (Mattinson,
⁴² 2005). U-Pb dates developed using these methods have led to an updated chronostratigraphic

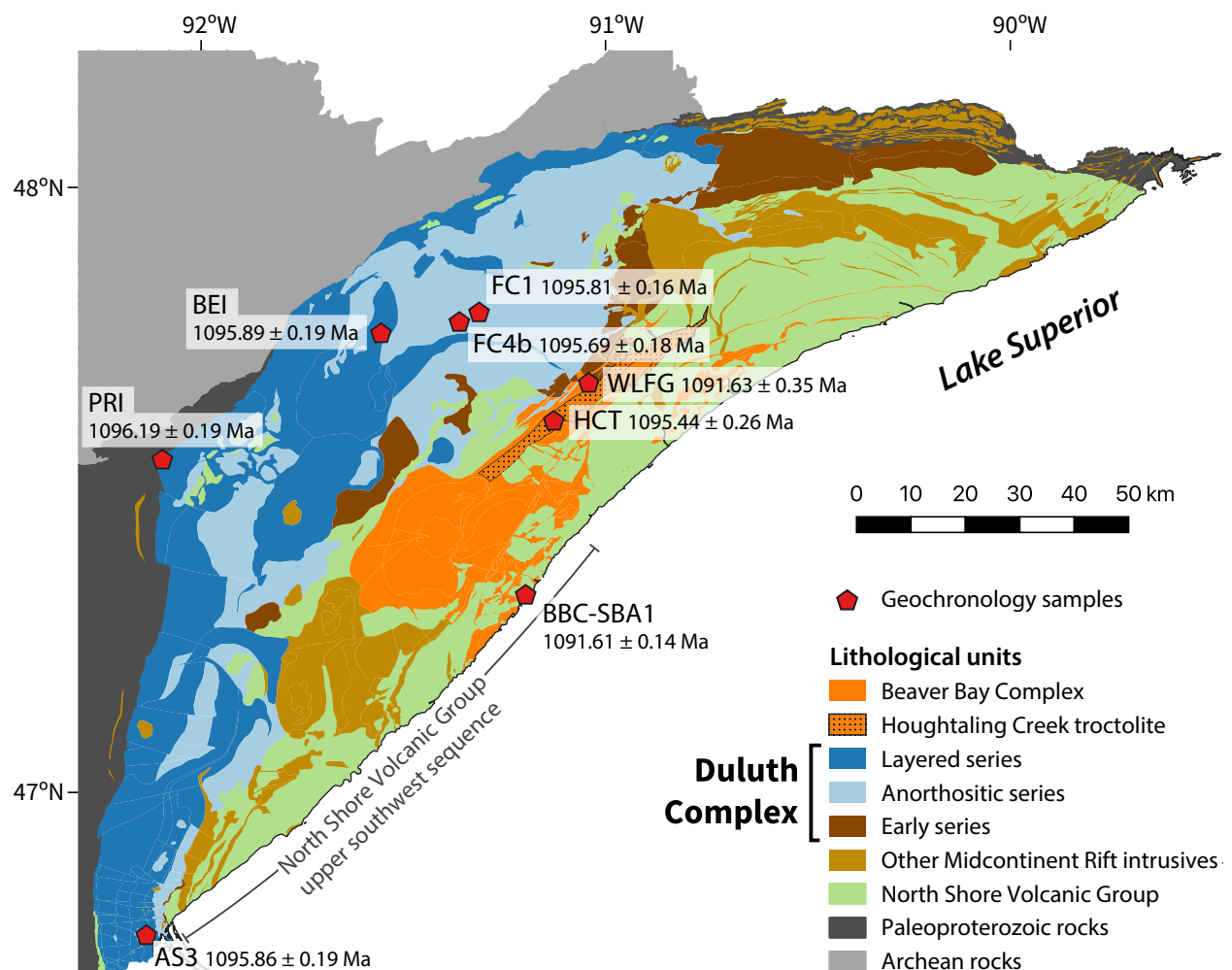


Figure 1. Geologic map of NE Minnesota (simplified from Jirsa et al., 2011) highlighting Midcontinent Rift intrusive complexes and geochronology sample locations. Volcanic and intrusive units dip towards Lake Superior typically at 10° to 20° . U-Pb dates from the anorthositic and layered series of the Duluth Complex (light and dark blue) indicate rapid emplacement in less than 1 million years.

43 framework for Midcontinent Rift volcanics (Swanson-Hysell et al., 2019; Fig. 2). With these
 44 higher precision constraints, the timing and tempo of magmatic activity within the rift can be
 45 reevaluated – was it continuous or punctuated by pulses? Key to evaluating this question is the
 46 timing of emplacement of intrusive rocks, particularly the largest intrusive suite – the Duluth
 47 Complex (Fig. 1). With its arcuate area of 5630 km^2 , the tholeiitic Duluth Complex is the
 48 second-largest exposed mafic intrusive complex on Earth (Miller et al., 2002). It was emplaced as
 49 sheet-like intrusions into the base of a comagmatic volcanic succession with the majority of its

50 volume associated with the anorthositic series and the layered series of gabbroic and troctolitic
51 cumulates (Miller et al., 2002; Fig. 1). We present $^{206}\text{Pb}/^{238}\text{U}$ zircon dates from the Duluth
52 Complex, as well as the Beaver Bay Complex (Fig. 1), to improve constraints on the duration of
53 intrusive magmatism and contextualize it with the chronology of volcanism.

54 METHODS and RESULTS

55 Zircon crystals were chemically abraded prior to analysis by isotope dilution thermal ionization
56 mass spectrometry (ID-TIMS).¹ Weighted means were calculated from multiple single zircon
57 dates (Fig. 2 and Table 1). These $^{206}\text{Pb}/^{238}\text{U}$ dates can be compared to one another, and to the
58 volcanic dates of Swanson-Hysell et al. (2019), at the level of analytical uncertainty (X uncertainty
59 in Table 1) given that all dates were developed using EARTHTIME tracer solutions (Condon
60 et al., 2015). This 2σ analytical uncertainty will be reported when dates are discussed. External
61 uncertainties and mean squared weighted deviation (MSWD) values are reported in Table 1.

62 The Duluth Complex anorthositic series comprises plagioclase-rich gabbroic cumulates varying
63 from anorthositic gabbro to anorthosite. Samples FC1 and FC4b are from gabbroic anorthosite
64 exposures near the former logging town of Forest Center (Minnesota). A weighted mean
65 $^{206}\text{Pb}/^{238}\text{U}$ date for FC1 of 1095.81 ± 0.16 Ma is calculated based on 10 single zircon dates
66 (Table 1). This date is indistinguishable from a weighted mean $^{206}\text{Pb}/^{238}\text{U}$ date for FC1 of
67 1095.97 ± 0.22 Ma developed by Ibañez-Mejia and Tissot (2019). Our new FC4b date is
68 indistinguishable from these FC1 dates with a weighted mean $^{206}\text{Pb}/^{238}\text{U}$ date of 1095.69 ± 0.18
69 Ma based on dates from 7 zircons. These dates are indistinguishable from the weighted mean
70 $^{206}\text{Pb}/^{238}\text{U}$ date of 1095.86 ± 0.19 Ma developed from chemically-abraded zircons of anorthositic

¹Supplemental Material. Individual zircon dates, paleomagnetic site mean directions, and additional method details. Please visit <https://doi.org/10.1130/GEOL.S.12935057> to access the supplemental material, and contact editing@geosociety.org with any questions. Paleomagnetic data and interpreted directions are available in the Magnetics Information Consortium (MagIC) database (<https://earthref.org/MagIC/doi/10.1130/G47873.1>). Geochronological data are available at <https://www.geochron.org> associated with International Geosample Numbers (IENSH000H, IENSH000I, IENSH000J, IENSH000K, IENSH000L and IENSH000M). Code associated with statistical tests and data visualization is available in a Zenodo repository <https://doi.org/10.5281/zenodo.4012382>.

71 series sample AS3 collected in the city of Duluth (Schoene et al., 2006; Fig. 2, Table 1). Zircon
 72 grains from these anorthositic series samples are commonly used as U-Pb standards.

73 The layered series of the Duluth Complex is a suite of stratiform troctolitic to gabbroic
 74 cumulates emplaced as discrete intrusions (Fig. 1). The PRI sample is an augite troctolite from
 75 the Partridge River intrusion which is at the base of the complex in contact with underlying
 76 Paleoproterozoic metasedimentary rocks (Fig. 1). Data from 6 zircons result in a weighted mean
 77 $^{206}\text{Pb}/^{238}\text{U}$ date of 1096.19 ± 0.19 Ma (Fig. 2). The BEI sample is an olivine gabbro from the
 78 Bald Eagle intrusion. This intrusion has been interpreted as one of the youngest layered series
 79 units based on cross-cutting relationships inferred from aeromagnetic data (Miller et al., 2002).
 80 Dates from 6 zircons of BEI result in a weighted mean $^{206}\text{Pb}/^{238}\text{U}$ date of 1095.89 ± 0.19 Ma
 81 (Fig. 2).

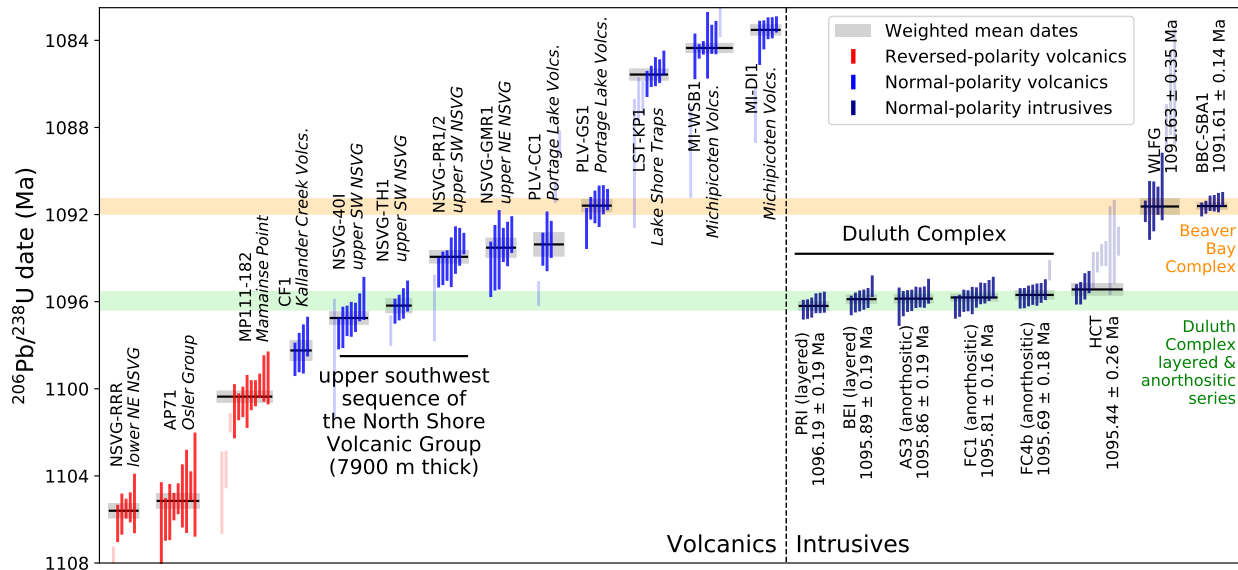


Figure 2. Date bar plot of CA-ID-TIMS $^{206}\text{Pb}/^{238}\text{U}$ zircon dates for Midcontinent Rift volcanics and intrusives. Dates for volcanics and BBC-SBA1 are from Fairchild et al. (2017) and Swanson-Hysell et al. (2019). The AS3 date is from Schoene et al. (2006). Each vertical bar represents the date for an individual zircon while the horizontal lines and grey boxes represent the weighted means and their uncertainty. The dates are colored by the geomagnetic polarity recorded by the unit or sequence of lavas. NSVG –North Shore Volcanic Group; Volcs. – Volcanics.

82 The Beaver Bay complex is a suite of dominantly hypabyssal intrusions that cross-cut the

83 North Shore Volcanic Group (Fig. 1). Sample HCT is an augite troctolite from the Houghtaling
84 Creek troctolite macrodike (Miller et al., 2001). In contrast to the internally-consistent dates
85 from the layered and anorthositic series samples, $^{206}\text{Pb}/^{238}\text{U}$ zircon dates from HCT have more
86 dispersion that we interpret as resulting from Pb loss not fully mitigated by chemical abrasion.
87 After excluding individual dates that trend away from concordia, dates from 4 concordant zircons
88 result in a weighted mean $^{206}\text{Pb}/^{238}\text{U}$ date of 1095.44 ± 0.26 Ma (Fig. 2). A sample of ferrodiorite
89 was collected as WLFG from the Wilson Lake ferrogabbro of the Beaver Bay Complex. This
90 plug-shaped zoned intrusion was emplaced into the Duluth Complex roof zone. Variable intensity
91 chemical abrasion was applied to WLFG zircons with hotter and longer dissolution yielding more
92 concordant data with older $^{206}\text{Pb}/^{238}\text{U}$ dates (Table S1 in the Supplemental Material). After
93 excluding those interpreted to have unmitigated Pb loss, dates from 5 zircons result in a weighted
94 mean $^{206}\text{Pb}/^{238}\text{U}$ date of 1091.63 ± 0.35 Ma (Fig. 2). This date is indistinguishable from the
95 1091.61 ± 0.14 Ma $^{206}\text{Pb}/^{238}\text{U}$ date developed from an aplite within a Silver Bay intrusion of the
96 Beaver Bay Complex (sample BBC-SBA1 of Fairchild et al., 2017; Figs. 1 and 2).

97 Paleomagnetic data from the layered series (37 sites) and the anorthositic series (11 sites) near
98 Duluth were published in Beck (1970) (Fig. 3). Site directions of the layered and anorthositic
99 series share a common mean, consistent with their overlapping U-Pb dates. In order to pair
100 paleomagnetic data with geochronology, oriented cores were collected and analyzed from the sites
101 of FC1, FC4 and HCT. Magnetization was measured on a 2G DC-SQUID magnetometer at UC
102 Berkeley. Samples underwent alternating field (AF) or thermal demagnetization steps and fits
103 were made using PmagPy software (Tauxe et al., 2016). While Beck (1970) did not implement tilt
104 corrections, the Duluth Complex and overlying lavas dip towards Lake Superior and
105 paleomagnetic data need to be corrected for this tilt. We compile abundant igneous layering
106 orientations, which are similar to the tilt of overlying lavas and interflow sediments, and use them
107 for tilt correction.

108 Rapid progression of poles within the apparent polar wander path (APWP) enable these

Table 1. Summary of CA-ID-TIMS $^{206}\text{Pb}/^{238}\text{U}$ dates from Midcontinent Rift intrusions

Sample	Group	Latitude Longitude	$^{206}\text{Pb}/^{238}\text{U}$ date (Ma)	Uncertainty (2σ)			MSWD	n/N
				X	Y	Z		
PRI <i>Partridge River Intrusion augite troctolite</i>	Duluth Complex (layered series)	47.5480° N 92.1074° W	1096.19	0.19	0.36	1.15	0.45	6/6
BEI <i>Bald Eagle Intrusion olivine gabbro</i>	Duluth Complex (layered series)	47.7516° N 91.5680° W	1095.89	0.19	0.36	1.15	1.59	6/6
AS3 <i>Duluth gabbroic anorthositic</i>	Duluth Complex (anorthositic series)	46.7621° N 92.1590° W	1095.86	0.19	0.36	1.15	0.43	8/8
FC1 <i>Forest Center gabbroic anorthosite</i>	Duluth Complex (anorthositic series)	47.7827° N 91.3266° W	1095.81	0.16	0.34	1.14	1.44	10/10
FC4b <i>Forest Center gabbroic anorthosite</i>	Duluth Complex (anorthositic series)	47.7677° N 91.3753° W	1095.69	0.18	0.35	1.14	0.34	7/8
HCT <i>Houghtaling Creek Troctolite</i>	Beaver Bay Complex	47.6009° N 91.1497° W	1095.44	0.26	0.40	1.16	1.13	4/11
WLFG <i>Wilson Lake Ferrogabbro ferrodiorite</i>	Beaver Bay Complex	47.6620° N 91.0619° W	1091.63	0.35	0.46	1.18	0.74	5/8
BBC-SBA1 <i>Silver Bay aplite</i>	Beaver Bay Complex	47.3143° N 91.2281° W	1091.61	0.14	0.30	1.2	1.0	6/6

Notes: X is 2σ analytical uncertainty; Y is 2σ uncertainty also incorporating tracer calibration for comparison to U-Pb dates not developed using EARTHTIME-calibrated tracer solutions; Z is 2σ uncertainty including X and Y, as well as ^{238}U decay constant uncertainty (0.108%; Jaffey et al., 1971). This Z uncertainty needs to be utilized when comparing to dates using other decay systems (e.g., $^{40}\text{Ar}/^{39}\text{Ar}$, $^{187}\text{Re}-^{187}\text{Os}$); MSWD is the mean squared weighted deviation; n is the number of individual zircon dates included in the calculated sample mean date; N is the number of individual zircons analyzed for the sample. All dates are from this study with the exceptions of samples AS3 (Schoene et al., 2006) and BBC-SBA1 (Fairchild et al., 2017).

109 paleomagnetic data to give chronological insight. Pole positions from the early stage of rift
 110 magmatism are different from those of main stage lavas (Fig. 3). The similar position of Duluth
 111 Complex layered and anorthositic series virtual geomagnetic poles (VGPs) is consistent with
 112 contemporaneous emplacement and they can be combined into a mean pole (Fig. 3). This pole
 113 can be compared to a synthesized APWP developed using an Euler pole inversion of
 114 chronostratigraphically-controlled volcanic poles (Swanson-Hysell et al., 2019). The Duluth
 115 Complex pole lies between the 1100 Ma and 1095 Ma path positions with the A_{95} uncertainty of
 116 the pole overlapping with the two angular standard deviations ellipse of the 1095 Ma path
 117 position. This result is consistent with a ca. 1096 Ma age for the layered and anorthositic series
 118 and strengthens the correlation with the volcanics.

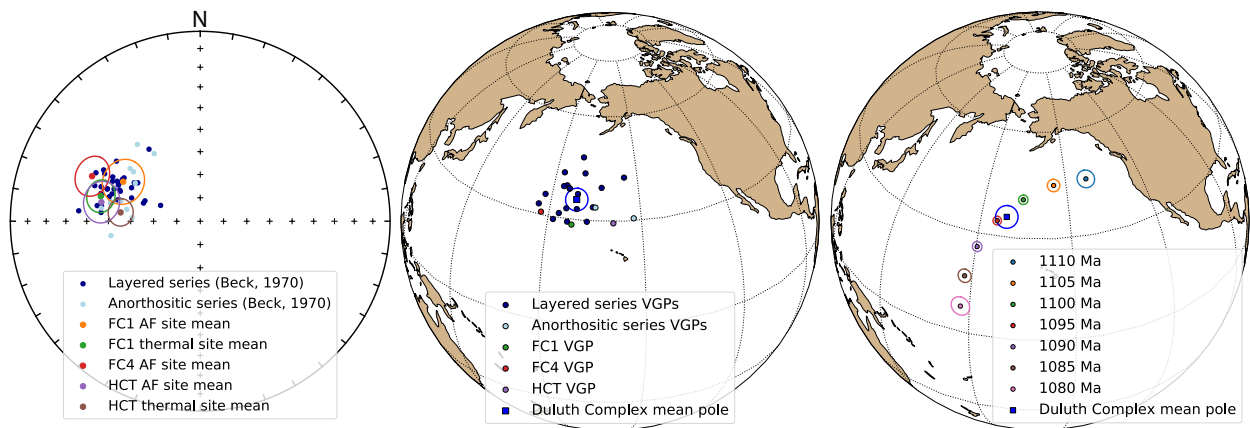


Figure 3. Left panel: tilt-corrected site mean paleomagnetic directions from anorthositic and layered series sites of Beck (1970) and from the FC1, FC4, and HCT sites. Center panel: Virtual geomagnetic poles (VGPs) for sites with 95% confidence angle $\alpha_{95} < 15^\circ$ give a mean pole of: 188.7° E, 35.6° N, $N=24$, $A_{95}=3.1$, $k=92$. Right panel: Duluth Complex pole shown with a synthesized pole path developed from Midcontinent Rift (MCR) volcanic poles.

119 DISCUSSION

120 Our new U-Pb dates, together with paleomagnetic data, imply that the bulk of the Duluth
 121 Complex layered series and anorthositic series were emplaced in less than 1 million years. The age
 122 differences between the anorthositic series and BEI layered series dates are all within uncertainty
 123 of no difference. The Partridge River intrusion layered series date is slightly older with an age
 124 difference from the rest of the anorthositic and layered series dates that is distinct from zero at
 125 95% confidence. Taking this oldest date of 1096.19 ± 0.19 Ma for PRI and the youngest date of
 126 1095.69 ± 0.18 Ma from FC4b yields a duration of overall emplacement of the layered and
 127 anorthositic series of $500,000 \pm 260,000$ years (2σ). This emplacement was coeval with eruption of
 128 the North Shore Volcanic Group (NSVG) upper southwest sequence which comprises ~ 7900
 129 meters of lavas and is the thickest exposed Midcontinent Rift volcanic succession (Fig. 1; Green
 130 et al., 2011; Swanson-Hysell et al., 2019). This rapid emplacement of the bulk of the Duluth
 131 Complex, together with coeval NSVG eruptions, require a large pulse of melt generation *ca.* 1096
 132 Ma.

133 The 1095.44 ± 0.26 Ma age of the Houghtaling Creek troctolite is indistinguishable from the

134 youngest Duluth Complex anorthositic series date. This result indicates that this pulse of
135 voluminous magmatic activity is represented in some Beaver Bay Complex intrusions. A younger
136 pulse of Beaver Bay Complex magmatism postdates NSVG eruptions, evidenced by units such as
137 the Silver Bay intrusions penetrating the youngest NSVG lavas, including the 1093.94 ± 0.28 Ma
138 Palisade Rhyolite (Miller et al., 2001; Swanson-Hysell et al., 2019; Fig. 1). The age of this
139 magmatism is constrained by indistinguishable dates of 1091.63 ± 0.35 Ma for the Wilson Lake
140 ferrogabbro and 1091.61 ± 0.14 Ma from the Silver Bay intrusions (Fig. 2; Table 1). This younger
141 Beaver Bay Complex magmatism is coeval with eruption of the >5 km thick Portage Lake
142 Volcanics that are exposed to the east on the Keweenaw Peninsula and Isle Royale in Michigan
143 (Fig. 2).

144 Rapid emplacement of the voluminous layered and anorthositic series of the Duluth Complex
145 bears similarities to the geologically short duration (<1 Myr) of well-dated flood basalt provinces
146 (Burgess et al., 2015; Schoene et al., 2019). This similarity supports the hypothesis put forward
147 by Green (1983), and advanced by others including Cannon and Hinze (1992) and Stein et al.
148 (2015), that co-location of massive magmatism and rifting is the result of lithospheric extension
149 atop decompression melting of an upwelling mantle plume. Contemporaneous heating of
150 Laurentia lithosphere 600 km to the north of the rift is indicated by thermochronologic data from
151 middle to lower crustal xenoliths (Edwards and Blackburn, 2018). Basaltic magma was also
152 emplaced throughout the Southwestern Laurentia large igneous province coeval with rift
153 magmatism, including sills >2300 km to the southwest of Duluth (Bright et al., 2014). That such
154 a broad region of Laurentia lithosphere experienced heating and magmatism supports
155 hypothesized large-scale mantle upwelling.

156 Both the *ca.* 1108 Ma early stage and *ca.* 1096 Ma main stage magmatic intervals within the
157 Midcontinent Rift were voluminous and have been interpreted to be the result of a plume-related
158 thermal anomaly. The interpretation that this volcanism is associated with a deep-seated mantle
159 plume needs to be reconciled with the long duration of magmatism and rapid equatorward motion

of Laurentia from a latitude of \sim 54° N *ca.* 1108 Ma during early stage flood basalt eruptions to \sim 32° N by *ca.* 1096 Ma (paleolatitudes for Duluth, MN). While some motion could be associated with true polar wander, in which the mesosphere and asthenosphere rotated in conjunction with the lithosphere, paleomagnetic pole positions require a substantial component of plate tectonic motion (Swanson-Hysell et al., 2019). The pulsed nature of magmatic activity could support an interpretation of multiple upwelling pulses. As postulated by Cannon and Hinze (1992), the initial pulse expressed by *ca.* 1108 early stage flood basalt volcanism initiated lithospheric thinning. Given the significantly thinned lithosphere in the Midcontinent Rift region, subsequent positively-buoyant plume material that encountered Laurentia lithosphere would have experienced “upside-down” drainage wherein relief at the base of the lithosphere resulted in lateral and upward flow into the Midcontinent Rift (Sleep, 1997; Swanson-Hysell et al., 2014). Flow of upwelling mantle to locally-thin lithosphere would have led to ponding and concentrated decompression melting within the rift. One scenario is that Laurentia was migrating over a plume generation zone (Burke et al., 2008) from which multiple deep-seated mantle plumes upwelled and reached the lithosphere during rift development. The first could have been centered on the present-day Lake Superior region with the second encountering Laurentian lithosphere and being directed to the rift by upside-down drainage in addition to driving magmatism in southwest Laurentia. Another scenario is that *ca.* 1096 Ma magmatism was invigorated by upwelling return flow enhanced by slab avalanche induced downwelling connected to the rapid plate motion of Laurentia that initiated in the early stage (Swanson-Hysell et al., 2019). Overall, the constraint that both the anorthositic and layered series of the Duluth Complex were emplaced in less than 1 million years requires an exceptional thermal anomaly that led to rapid and voluminous melt generation during the main stage of Midcontinent Rift development.

ACKNOWLEDGEMENTS

Project research was supported by U.S. National Science Foundation (NSF) grant EAR-1847277 (to NLS-H) and the University of Minnesota Duluth. Funding for Boise State Isotope Geology

186 Laboratory analytical infrastructure was provided by NSF grants EAR-0824974 and
187 EAR-0521221. Margaret Avery and Dan Costello provided field assistance. Constructive reviews
188 by Mauricio Ibañez-Mejia, Kyle Samperton, and an anonymous reviewer improved the manuscript.

189 References

- 190 Beck, M., 1970, Paleomagnetism of Keweenawan intrusive rocks, Minnesota: *Journal of Geophysical Research*,
191 vol. 75, pp. 4985–4996, doi:10.1029/JB075i026p04985.
- 192 Blackburn, T. J., Olsen, P. E., Bowring, S. A., McLean, N. M., Kent, D. V., Puffer, J., McHone, G., Rasbury, E. T.,
193 and Et-Touhami, M., 2013, Zircon U-Pb geochronology links the end-Triassic extinction with the Central
194 Atlantic Magmatic Province: *Science*, vol. 340, pp. 941–945, doi:10.1126/science.1234204.
- 195 Bright, R. M., Amato, J. M., Denyszyn, S. W., and Ernst, R. E., 2014, U-Pb geochronology of 1.1 Ga diabase in the
196 southwestern United States: Testing models for the origin of a post-Grenville large igneous province:
197 *Lithosphere*, vol. 6, pp. 135–156, doi:10.1130/L335.1.
- 198 Burgess, S. D., Bowring, S. A., Fleming, T. H., and Elliot, D. H., 2015, High-precision geochronology links the
199 Ferrar large igneous province with early-Jurassic ocean anoxia and biotic crisis: *Earth and Planetary Science
Letters*, vol. 415, pp. 90–99, doi:10.1016/j.epsl.2015.01.037.
- 200 Burke, K., Steinberger, B., Torsvik, T. H., and Smethurst, M. A., 2008, Plume generation zones at the margins of
201 large low shear velocity provinces on the core–mantle boundary: *Earth and Planetary Science Letters*, vol. 265,
202 pp. 49–60, doi:10.1016/j.epsl.2007.09.042.
- 203 Cannon, W. F., 1992, The Midcontinent rift in the Lake Superior region with emphasis on its geodynamic
204 evolution: *Tectonophysics*, vol. 213, pp. 41–48, doi:10.1016/0040-1951(92)90250-A.
- 205 Cannon, W. F. and Hinze, W. J., 1992, Speculations on the origin of the North American Midcontinent rift:
206 *Tectonophysics*, vol. 213, pp. 49–55, doi:10.1016/0040-1951(92)90251-Z.
- 207 Condon, D. J., Schoene, B., McLean, N. M., Bowring, S. A., and Parrish, R. R., 2015, Metrology and traceability of
208 U–Pb isotope dilution geochronology (EARTHTIME tracer calibration part I): *Geochimica et Cosmochimica
Acta*, vol. 164, pp. 464–480, doi:10.1016/j.gca.2015.05.026.
- 209 Davis, D. and Green, J., 1997, Geochronology of the North American Midcontinent rift in western Lake Superior
210 and implications for its geodynamic evolution: *Canadian Journal of Earth Science*, vol. 34, pp. 476–488,
211 doi:10.1139/e17-039.
- 212 Edwards, G. H. and Blackburn, T., 2018, Detecting the extent of ca. 1.1 Ga Midcontinent Rift plume heating using
213 U-Pb thermochronology of the lower crust: *Geology*, vol. 46, pp. 911–914, doi:10.1130/g45150.1.
- 214 Fairchild, L. M., Swanson-Hysell, N. L., Ramezani, J., Sprain, C. J., and Bowring, S. A., 2017, The end of
215 Midcontinent Rift magmatism and the paleogeography of Laurentia: *Lithosphere*, vol. 9, pp. 117–133,
216 doi:10.1130/L580.1.
- 217 Green, J., 1983, Geologic and geochemical evidence for the nature and development of the Middle Proterozoic
218 (Keweenawan) Midcontinent Rift of North America: *Tectonophysics*, vol. 94, pp. 413–437,
219 doi:10.1016/0040-1951(83)90027-6.
- 220 Green, J. C., Boerboom, T. J., Schmidt, S. T., and Fitz, T. J., 2011, The North Shore Volcanic Group:
221 Mesoproterozoic plateau volcanic rocks of the Midcontinent Rift System in northeastern Minnesota: *GSA Field
Guides*, vol. 24, pp. 121–146, doi:10.1130/2011.0024(07).

- 225 Ibañez-Mejia, M. and Tissot, F. L. H., 2019, Extreme Zr stable isotope fractionation during magmatic fractional
226 crystallization: *Science Advances*, vol. 5, p. eaax8648, doi:10.1126/sciadv.aax8648.
- 227 Jaffey, A., Flynn, K., Glendenin, L., Bentley, W., and Essling, A., 1971, Precision measurement of half-lives and
228 specific activities of ^{235}U and ^{238}U : *Physical Review*, vol. C4, pp. 1889–1906, doi:10.1103/PhysRevC.4.1889.
- 229 Jirsa, M. A., Boerboom, T., Chandler, V., Mossler, J., Runkel, A., and Setterholm, D., 2011, S-21 Geologic map of
230 Minnesota-bedrock geology: Tech. rep., Minnesota Geological Survey, URL
231 <http://hdl.handle.net/11299/101466>.
- 232 Mattinson, J. M., 2005, Zircon U/Pb chemical abrasion (CA-TIMS) method: Combined annealing and multi-step
233 partial dissolution analysis for improved precision and accuracy of zircon ages: *Chemical Geology*, vol. 220, pp.
234 47–66, doi:10.1016/j.chemgeo.2005.03.011.
- 235 Miller, J., James D., Green, J. C., Severson, M. J., Chandler, V. W., and Peterson, D. M., 2001, M-119 Geologic
236 map of the Duluth Complex and related rocks, northeastern Minnesota: Tech. rep., Minnesota Geological Survey.
- 237 Miller, J., J.D., Green, J., Severson, M., Chandler, V., Hauck, S., Peterson, D., and Wahl, T., 2002, Geology and
238 mineral potential of the Duluth Complex and related rocks of northeastern Minnesota: Minnesota Geological
239 Survey Report of Investigations, vol. 58.
- 240 Nicholson, S. W. and Shirey, S. B., 1990, Midcontinent Rift Volcanism in the Lake Superior Region: Sr, Nd, and Pb
241 Isotopic Evidence for a Mantle Plume Origin: *J. Geophys. Res.*, vol. 95, pp. 10,851–10,868,
242 doi:10.1029/JB095iB07p10851.
- 243 Paces, J. and Miller, J., 1993, Precise U-Pb ages of Duluth Complex and related mafic intrusions, northeastern
244 Minnesota: Geochronological insights to physical, petrogenetic, paleomagnetic and tectonomagmatic processes
245 associated with the 1.1 Ga Midcontinent Rift System: *Journal of Geophysical Research*, vol. 98, pp.
246 13,997–14,013, doi:10.1029/93jb01159.
- 247 Schoene, B., Crowley, J. L., Condon, D. J., Schmitz, M. D., and Bowring, S. A., 2006, Reassessing the uranium
248 decay constants for geochronology using ID-TIMS U–Pb data: *Geochimica et Cosmochimica Acta*, vol. 70, pp.
249 426–445, doi:10.1016/j.gca.2005.09.007.
- 250 Schoene, B., Eddy, M. P., Samperton, K. M., Keller, C. B., Keller, G., Adatte, T., and Khadri, S. F. R., 2019, U-Pb
251 constraints on pulsed eruption of the Deccan Traps across the end-Cretaceous mass extinction: *Science*, vol. 363,
252 pp. 862–866, doi:10.1126/science.aau2422.
- 253 Sleep, N. H., 1997, Lateral flow and ponding of starting plume material: *Journal of Geophysical Research: Solid*
254 *Earth*, vol. 102, pp. 10,001–10,012, doi:10.1029/97JB00551.
- 255 Sprain, C. J., Renne, P. R., Vanderkluysen, L., Pande, K., Self, S., and Mittal, T., 2019, The eruptive tempo of
256 Deccan volcanism in relation to the Cretaceous-Paleogene boundary: *Science*, vol. 363, pp. 866–870,
257 doi:10.1126/science.aav1446.
- 258 Stein, C. A., Kley, J., Stein, S., Hindle, D., and Keller, G. R., 2015, North America's Midcontinent Rift: When rift
259 met LIP: *Geosphere*, doi:10.1130/GES01183.1.
- 260 Swanson-Hysell, N. L., Ramezani, J., Fairchild, L. M., and Rose, I. R., 2019, Failed rifting and fast drifting:
261 Midcontinent Rift development, Laurentia's rapid motion and the driver of Grenvillian orogenesis: *GSA Bulletin*,
262 doi:10.1130/b31944.1.
- 263 Swanson-Hysell, N. L., Vaughan, A. A., Mustain, M. R., and Asp, K. E., 2014, Confirmation of progressive plate
264 motion during the Midcontinent Rift's early magmatic stage from the Osler Volcanic Group, Ontario, Canada:
265 *Geochemistry Geophysics Geosystems*, vol. 15, pp. 2039–2047, doi:10.1002/2013GC005180.

- 266 Tauxe, L., Shaar, R., Jonestrask, L., Swanson-Hysell, N., Minnett, R., Koppers, A., Constable, C., Jarboe, N.,
267 Gaastra, K., and Fairchild, L., 2016, PmagPy: Software package for paleomagnetic data analysis and a bridge to
268 the Magnetics Information Consortium (MagIC) Database: *Geochemistry, Geophysics, Geosystems*,
269 doi:10.1002/2016GC006307.
- 270 Vervoort, J., Wirth, K., Kennedy, B., Sandland, T., and Harpp, K., 2007, The magmatic evolution of the
271 Midcontinent rift: New geochronologic and geochemical evidence from felsic magmatism: *Precambrian Research*,
272 vol. 157, pp. 235–268, doi:10.1016/j.precamres.2007.02.019.
- 273 White, R. and McKenzie, D., 1995, Mantle plumes and flood basalts: *Journal of Geophysical Research: Solid Earth*
274 (1978–2012), vol. 100, pp. 17,543–17,585, doi:10.1029/95JB01585.